Journal of Engineering and Applied Research (JEAR)
National University of Skill
Winter & Spring 2026, Vol. 3, No. 1, p. ..-..
Journal Homepage: https://jear.tvu.ac.ir
:10.48301/vjtve.2026.517582.1112

Investigation of the Effect of Changes in Coolant Pressure on Local Boiling in Engine

Hadi Ghasemi Zavaragh [1*], Bahman Rahmatinejad [2]

[1, 2] Department of Mechanical Engineering, Technical and Vocational University (TVU), Tehran, Iran.

ARTICLE INFO

Article Type:
Original Research

Received: 2025.04.19
Revised: 2025.11.01
Accepted: 2026.05.17

Keyword:
Engine
Cooling system
Local boiling
Pressure changes

***Corresponding Author:**
Hadi Ghasemi Zavaragh
Email: *haghasemi@tvu.ac.ir*

ABSTRACT

The cooling system is essential for the optimal operation of internal combustion engines. Regular maintenance and monitoring can enhance its performance and extend the engine's lifespan. This study examined the effect of changes in coolant pressure on local boiling in the Ford MVH418 engine. Tests were conducted at eight different speeds and two loads of 15% and 30%. A Cussons dynamometer was used to measure load and torque. Coolant pressure was measured at three points: the inlet and outlet of the radiator and the engine inlet, using an MPS500 pressure sensor. Results indicated that at high RPMs and heavier loads, engine warm-up time is reduced. Additionally, the greatest pressure difference observed in all tests was between the radiator inlet and outlet, which increases with higher RPMs and applied loads. For example, at a load of 30%, this pressure difference reached a maximum of 10.6% at 1500 RPM and 38.3% at 3000 RPM.

E-ISSN: 3060-6357

1)Introduction

Internal combustion engines have widespread applications today. In this system, high-efficiency power generation depends on the correct functioning of all its parts. Heat transfer from the engine must be controlled and released to the environment at a specific temperature, ensuring that the temperature of various engine points does not exceed or fall below a certain limit. Given the sensitivity of temperatures at different points in internal combustion engines, the importance of heat transfer in these engines is very high [1].

The cooling system of an internal combustion engine is crucial for maintaining optimal operating temperatures and ensuring efficient engine performance. The main role of the cooling system is to dissipate the heat generated by the internal combustion engine during operation. If the engine overheats, it can lead to serious damage, such as a blown head gasket or head warping. The cooling system helps regulate engine temperature and prevents these problems. The antifreeze used in the coolant increases the boiling point of the liquid, allowing it to transfer more heat without turning into steam. This is crucial for preventing engine overheating. In cold climates, the antifreeze in the coolant prevents the liquid from freezing and lowers its freezing point. The coolant typically consists of water, ethylene glycol or propylene glycol, and various additives to prevent corrosion and improve system performance. This liquid circulates within the engine, absorbing heat, and then transfers it to the radiator for cooling. The radiator, usually located at the front of the vehicle, transfers heat from the coolant to the air and typically has a large surface area to increase heat exchange. A pump is used to circulate the coolant through the engine. This pump usually receives its power from the engine via a belt or chain [2].

It helps maintain a constant flow of coolant. In automobiles, a thermostat is used to regulate engine temperature. When the engine is cold, the thermostat remains closed to allow the engine to warm up faster, and when it reaches the desired temperature, it opens, allowing the coolant to flow to the radiator [3]. The presence of a thermostat reduces warm-up time. The process of heating the engine from a cold state to its optimal operating temperature is called warm-up. Numerous researchers have investigated automotive cooling systems. Some of these are mentioned below. In 2018, Shakeri and colleagues conducted a numerical simulation of subcooled flow boiling in the cooling passage of internal combustion engines through numerical modeling within a point-heated channel. In their research, they attempted to model subcooled boiling in a geometry similar to the water channel within an internal combustion engine using commercial software. The results showed that with increasing velocity, the effect of roughness decreased, and the numerical values approached the practical values. Also, as the surface temperature exceeded the saturation temperature, the heat transfer rate by this mechanism increased significantly [4].

In 2022, Shabani and colleagues conducted experimental and numerical simulations of flow and heat transfer in an automobile radiator under forced and natural convection. In the experimental solution, an aluminum automobile radiator with flowing coolant was examined under real boundary conditions during engine shutdown. The inlet and outlet temperatures of the radiator were measured using two negative temperature coefficient (NTC) thermistors. In the numerical analysis, the continuity, momentum, and energy equations were solved using the control volume method for numerical solution of the flow using ANSYS Fluent software. In this study, the effects of secondary flows, centrifugal force, and buoyancy on the flow field were considered. The effect of natural and forced convection on radiator heat transfer was also investigated. The results show that the inlet-outlet temperature difference in the engine under free circulation is 13°C in the experimental solution and 1.12°C in the numerical solution, and under forced fluid circulation, the inlet-outlet temperature difference in the engine is 1.5°C in the experimental solution and 1.8°C in the numerical solution [5]. Alalo et al. (2022) analyzed energy and exergy during the cold and warm-up phases of an engine. Since exergy analysis can qualitatively and quantitatively assess loss sources using the first and second laws of thermodynamics, this study investigated the impact of engine temperature on energy and exergy parameters during engine warm-up. Using a Cummins turbocharged engine, performance and emission data were measured, and energy and exergy parameters were extracted from the experimental data. Results showed that as the engine warmed up, fuel exergy, exhaust heat loss, and exergy destruction (referring to the amount of exergy lost in a system due to irreversibilities such as friction, mixing, chemical reactions, heat transfer, and uncontrolled expansion) decreased by 2.3%, 1.34%, and 1.34%, respectively; while exhaust exergy loss increased by 43.5% [6]. Etikyala et al. (2023) investigated soot formation during load changes in a single-cylinder GDI engine. The engine load was increased from 4 bar NMEP (Net Mean Effective Pressure) to a maximum of 12 bar NMEP in 2 seconds at an engine speed of 2000 rpm. During these changes, engine particulate matter emissions were measured in terms of particle number (PN), and images of the in-cylinder combustion process were recorded via an endoscope using a high-speed camera to identify soot formation locations. Tests were conducted at different coolant temperatures and using different injection strategies to determine how these parameters affect PN emissions. Coolant temperature was identified as the dominant factor in controlling PN emissions during transients [7]. Lee et al. (2024) investigated improving vehicle warm-up performance using phase-change materials and thermal energy storage methods. Their research aimed to utilize waste heat from engine cooling to improve cold-start performance, thereby reducing fuel consumption and emissions. A thermal energy storage device was designed and built. Results showed energy transfer of 591, 489, 446, and 315 kJ for 4, 8, 16, and 24 hours, respectively. Regarding warm-up time, using the thermal energy storage devices reduced the time to reach 70°C by 24.45%. This reduction in warm-up time directly contributed to faster engine stabilization and resulted in corresponding improvements in fuel efficiency and a reduction in exhaust emissions, including CO2 [8]. Redouane et al. (2024) conducted a review on automotive engine cooling systems, demonstrating that the use of nanofluids leads to improved convective heat transfer coefficients for all nanoparticle volume concentrations compared to water under various operating conditions. This study provides insights into the potential of nanofluids for enhancing cooling efficiency in automotive applications [9]. Chang et al. (2024) designed an advanced cooling system for gas engine vehicles. Their research presented an innovative algorithm that precisely activates the engine coolant flow at optimal times, thus protecting gas engines from catastrophic failures such as overheating [10].

Efficient thermal management remains a critical concern in modern internal combustion engines, as fluctuations in coolant pressure and temperature can induce localized boiling, resulting in hot spots, reduced heat transfer efficiency, and potential component degradation. This study presents an innovative experimental investigation into the influence of coolant pressure variations on local boiling behavior in the Ford MVH418 engine. Utilizing real-time pressure mapping and dynamic load simulations, the research examines how pressure changes affect coolant flow stability and radiator performance. Findings of this research provide valuable insights for the design of adaptive cooling systems that sustain optimal pressure and temperature conditions, thereby improving engine efficiency, reliability, and operational longevity.

2) Materials and Methods

2-1 Localized Boiling

Localized boiling refers to a phenomenon in which, in parts of the cooling system – usually near the very hot walls of the engine – the coolant (water or antifreeze solution) locally reaches its boiling point and turns into steam, while the overall system temperature has not yet reached the boiling point. The cause of localized boiling in the engine cooling system can be due to excessive increase in the metal surface temperature in areas such as around the exhaust valves or combustion chamber; a decrease in cooling system pressure; reduced coolant flow or clogged passages; or the use of unsuitable or worn-out coolant. This can have consequences such as disruption of heat transfer due to the formation of vapor bubbles on the metal surface; localized temperature increase and, ultimately, overall engine overheating.

Although the temperature of the fluid flowing over the wall surface of the engine is lower than the saturation temperature, boiling occurs at the wall surface because the wall temperature is very high. In such cases, heat energy is transferred directly from the wall to the engine cooling liquid. Some of the energy transferred to the liquid increases the temperature of the fluid, while another portion produces vapor. However, the fluid in the saturated vapor phase condenses, and the resulting interphase heat transfer also increases the average temperature of the liquid. Some of the energy is transferred directly from the wall to the fluid in the vapor phase.

Figure 1 illustrates how localized boiling occurs in the engine (hot spots, vapor formation, and heat flow disruption).

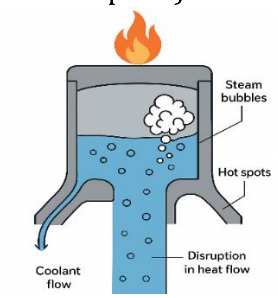

Figure 1. Localized Boiling in the Engine

This research utilized a four-cylinder Ford MVH418 engine mounted on a Cussons dynamometer. This dynamometer was used to simulate real-world engine operating conditions at different loads (15%, 30%). A dynamometer is a mechanical device used to measure force, torque, or power. Depending on the design, dynamometers can measure dynamic torque, steady-state power, or other performance metrics. The overall structure of the Cussons dynamometer used in this research includes several key components enabling efficient force, torque, and power measurement: a robust frame forming the main support, typically constructed from heavy-duty steel or other durable materials to withstand vibrations and forces; a rotating shaft, the main component transferring torque from the engine to the device, usually made of high-strength materials to withstand rotational forces without bending or breaking; a torque sensor to measure the torque applied to the rotating shaft, converting mechanical force into an electrical signal (various types of sensors, such as strain gauge-based load cells or other torque measurement technologies, can be used); a braking system providing resistance to the rotating shaft to create a controlled load on the tested engine; a control panel allowing the user to control the dynamometer, monitor performance, and read measurements; a data acquisition system collecting data from the load cell and other sensors and sending it to a separate computer system for analysis; and a cooling system used in extended tests to prevent overheating. Coolant pressure was measured at three points: the engine inlet, radiator inlet, and radiator outlet. The location of the pressure sensors is shown in Figure 2.

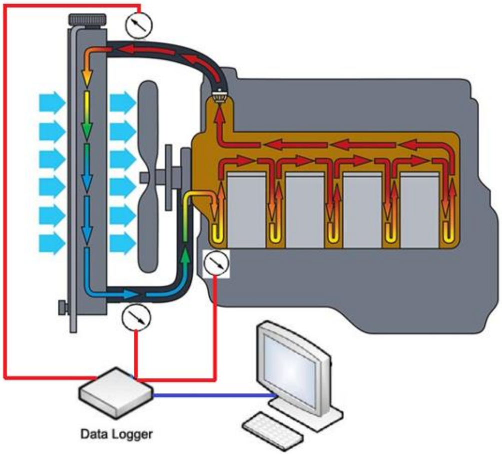

Figure 2. Location of pressure sensors on the engine

The engine has been analyzed at 8 speeds and various loads over a period of 15 minutes to examine the cooling system's performance very precisely. A control system was used to manage the throttle valve. The technical specifications of this engine are presented in Table 1.

Table 1. Technical specifications of the Ford MVH418 engine [11]

Engine	Ford MVH418
Cylinders	Four cylinders in line
Engine capacity	1.796 L
Cylinder bore (mm)	80.6
Stroke (mm)	88

Compression ratio	10
Maximum power (Kw)	77
Maximum torque (Nm)	153 (4000 rpm)
Idle speed	750 RPM
Maximum speed	5950 RPM

To measure the coolant pressure at different points in the engine (inlet and outlet of the radiator and engine inlet), the Mesens-MPS500-011 sensor was used, which has an uncertainty of ± 0.5%. This sensor is suitable for measuring the pressure of liquids and gases at high temperatures (Figure 3). It features high corrosion resistance, a wide measurement range, ease of assembly, and various output signals. The specifications of this sensor are provided in Table 2.

Figure 3. MPS500 sensor for pressure measurement

Table 2. Technical specifications of the MPS500 pressure sensor [12]

Connection	1/4", 1/2" NPT / G, M20x1,5
Measuring range	0...50 mBar - 0...1000 Bar
Output	4...20mA, 0-10VDC, 0-5 VDC, 1-5 VDC
Accuracy	<± 0,5 % F.S Opt; 0,2
Supply voltage	10 VDC ... 32VDC
Operating temperature	-40°C...+125 °C

Vibration and shock limitation	20g, 20...5000 Hz – 100g, 11 mSec
Hysteresis, repeatability	0,05% of FS
Zero adjustment	+/- 5 % full scale
Response time	4 mSec.

The coding of MPS model pressure sensors is as shown in Figure 4.

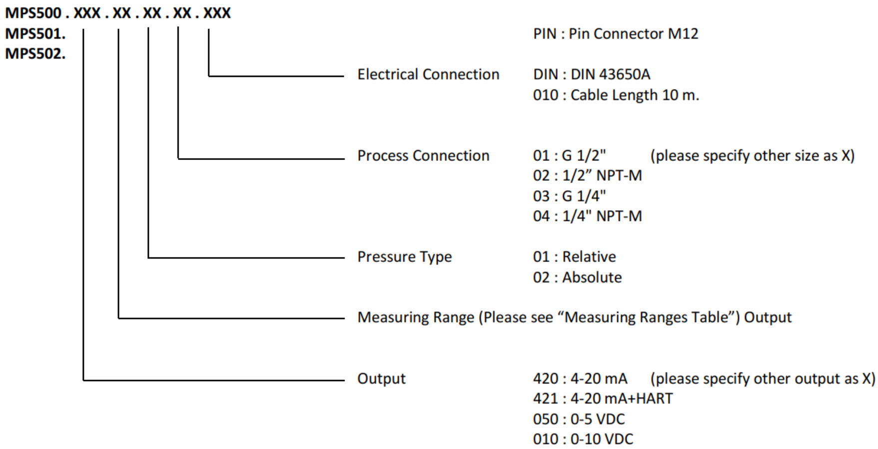

Figure 4. Coding of MPS model pressure sensors

2-2 Uncertainty analysis

The uncertainty in the plotted pressure curves can be expressed as a combined standard uncertainty consisting of at least two parts:

A: statistical uncertainty

B: instrument / systematic uncertainty

$$u_c(t) = \sqrt{u_A(t)^2 + u_B(t)^2} \quad (1)$$

where

$u_A(t)$ is the standard uncertainty of the mean pressure at time (t)

$u_B(t)$ is the standard uncertainty from instrument/spec.

Compute each term as follows:

From repeat measurements at time (t) (you have (n) repeated runs):

$$s(t) = \sqrt{\frac{1}{n-1}\sum_{i=1}^{n}(p_i(t) - \bar{p}(t))^2} \quad \text{(sample standard deviation)} \quad (2)$$

$$u_A(t) = \frac{s(t)}{\sqrt{n}} \quad \text{(standard uncertainty of the mean)} \tag{3}$$

From the instrument/specification: if the manufacturer gives a fixed half-width uncertainty ΔP (±0.5% bar) and you assume a rectangular distribution,

$$u_B(t) = \frac{\Delta P}{\sqrt{3}} \tag{4}$$

If the spec is a percentage α of the reading (±1% of (P)), then

$$u_B(t) = \frac{\alpha P(t)}{\sqrt{3}} \tag{5}$$

Combined:

$$u_c(t) = \sqrt{(\frac{s(t)}{\sqrt{n}})^2 + (\frac{\Delta P}{\sqrt{3}})^2} \tag{6}$$

(or substitute the percentage expression for ΔP).

For a confidence interval (expanded uncertainty) use an expansion factor (k) (commonly (k=2) for ≈95%):

$$U(t) = k u_c(t) \tag{7}$$

2-3 Heat transfer coefficient estimation

Estimating the thermal conductivity of a material is one of the key steps in heat transfer analyses and thermal system design. Use the Dittus–Boelter correlation for turbulent flow inside the cooling passages:

$$N_u = 0.023 Re^{0.8} Pr^{0.4} \tag{8}$$

Then,

$$h = \frac{Nu.k}{D_h} \tag{9}$$

$$R_e = \frac{\rho u D_h}{\mu} \tag{10}$$

$$P_r = \frac{C_p \mu}{k} \quad (11)$$

Where:
Nu: Nusselt number
Re: Reynolds number
Pr: Prandtl number
h: Convective heat transfer coefficient
D_h: Hydraulic diameter of coolant passage

We can relate the pressure difference between inlet and outlet to flow velocity (u) via the Darcy–Weisbach equation:

Combining these allows we to calculate h as a function of measured ΔP, providing a quantitative link between pressure data and cooling performance.

$$\Delta P = f \frac{L}{D_h} \frac{\rho u^2}{2} \quad (12)$$

3) Results and Discussion

3-1 First Test

In this test, the thermostat is removed from the engine, and since the engine is operating without a thermostat, the output pressure of the engine (radiator inlet) immediately increases as soon as it starts. The initial pressure increase in this test is due to the water pump pressure, but over time, we continue to observe an increase in pressure, which is attributed to the engine heating up and the rise in temperature. When the warm-up period of the engine ends, as the temperature stabilizes within a specific range, the rate of pressure increase decreases and reaches a constant value. In Figure 5, the X-axis component represents time, and the Y-axis component represents pressure. This figure illustrates pressure variations in three sensors: radiator input, radiator output, and engine input, across different speeds and loads. Additionally, it was observed from all three graphs that at higher RPMs and heavy loads, the warm-up time is shorter (Figure 5). In Figure 6, the uncertainty diagram of Figure 5-a was drawn.

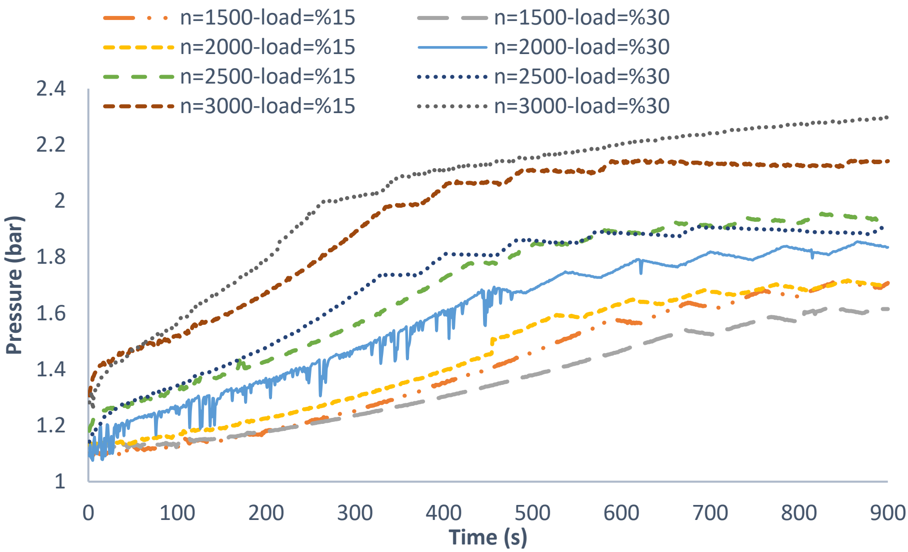
n=1500-load=%15
n=1500-load=%30
n=2000-load=%15
n=2000-load=%30
n=2500-load=%15
n=2500-load=%30
n=3000-load=%15
n=3000-load=%30
Pressure (bar)
2.4
2.2
2
1.8
1.6
1.4
1.2
1
0
100
200
300
400
500
600
700
800
900
Time (s)

(a)

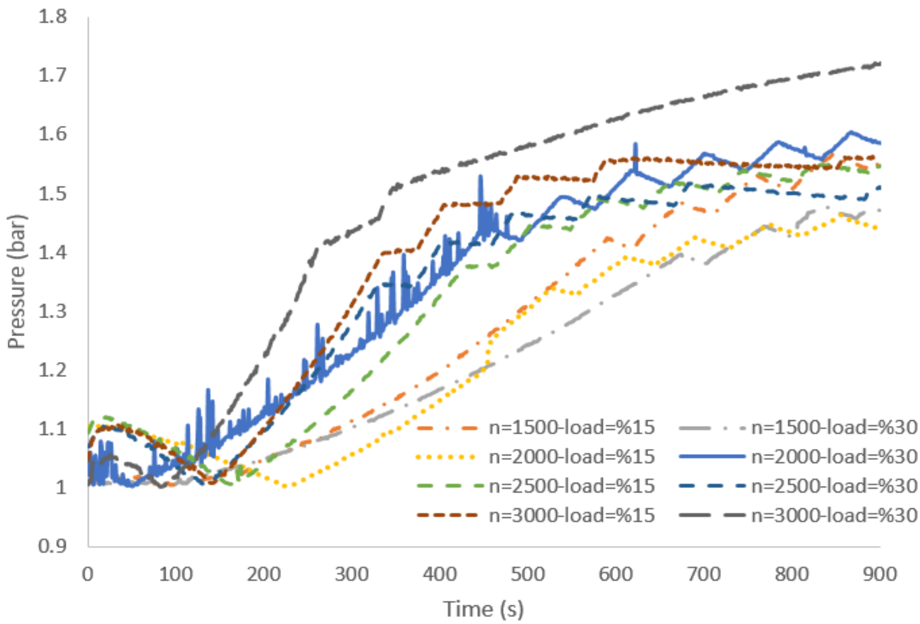
Pressure (bar)
1.8
1.7
1.6
1.5
1.4
1.3
1.2
1.1
1
0.9
n=1500-load=%15
n=1500-load=%30
n=2000-load=%15
n=2000-load=%30
n=2500-load=%15
n=2500-load=%30
n=3000-load=%15
n=3000-load=%30
0
100
200
300
400
500
600
700
800
900
Time (s)

(b)

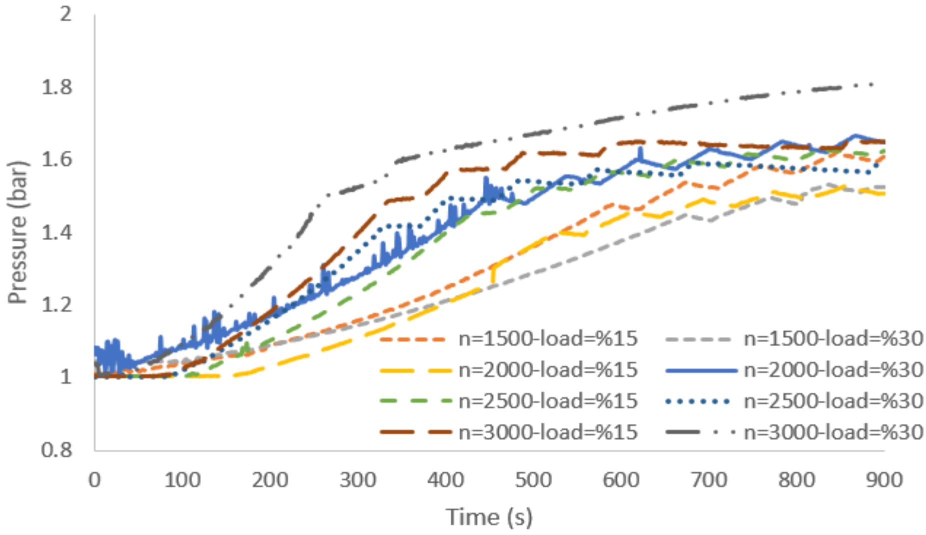

(c)

Figure 5. Comparison of coolant pressure in (a) radiator inlet, (b) radiator outlet, (c) engine inlet

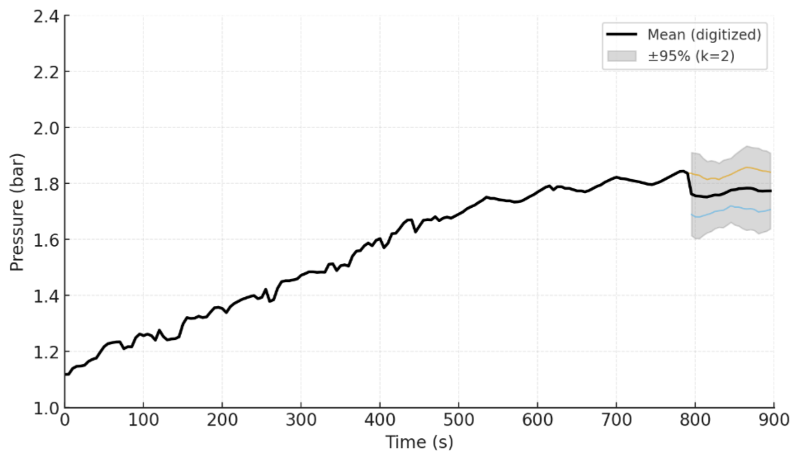

Figure 6: Uncertainty diagram for figure 4-a

In the diagram of Figure 7, the X-axis component represents time and the Y-axis component represents pressure. In this figure, pressure variations of three sensors were investigated at different speeds and loads. Ultimately, based on the graph in Figure 7, it can be concluded that the highest pressure is the engine output pressure (radiator inlet). The reasons for this can be summarized in two points:

a) The water pump takes the coolant from the radiator outlet and, after compression, sends it to the engine block, and this compressed flow exits from the engine outlet after passing through the engine block.

b) Due to the heat transferred from the engine to the coolant, the temperature of the fluid increases, and in some areas at higher RPMs and heavy loads, boiling occurs. For this reason, the engine output pressure is at its highest level.

The coolant that exits the engine is directly transferred to the radiator and, after cooling, returns from the radiator to the engine. As seen in Figure 7, the radiator outlet pressure is lower than its inlet pressure, and this is due to the decrease in pressure and temperature caused by the change in speed and temperature of the water as it enters the radiator through the capillary tubes, and this water returns to the engine block at a lower pressure and temperature.

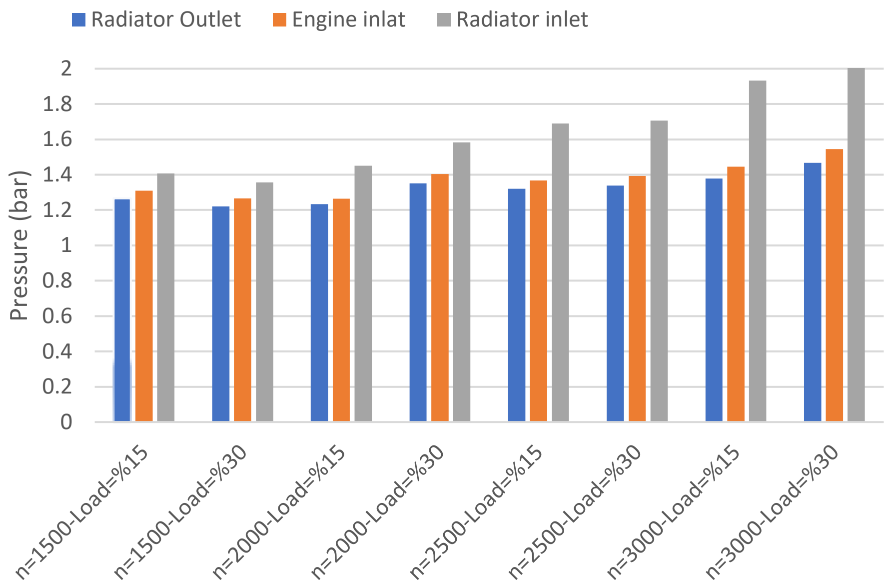

Figure 7. compares the average pressure of the coolant fluid at all three measurement points.

The greatest pressure difference observed in all tests relates to the pressure difference between the inlet and outlet of the radiator (Figure 7), which increases with the rise in RPM and load applied to the system. For example, this pressure difference at 1500 RPM and 30% load is a maximum of 6.10%, which increases to 38.3% at 3000 RPM and 30% load.

3-2 Second Test

In this test, a thermostat is used on the engine. Therefore, at the beginning of the test, due to the coolant fluid being cold and the thermostat being closed, the fluid does not circulate in the system, and an increase in pressure is not observed in the graphs of Figure 8. The addition of the thermostat to the system causes severe pressure fluctuations. In fact, these fluctuations are due to the continuous opening and closing of the thermostat. Additionally, the pressure in the cooling system decreases, which is due to the lack of continuous flow of coolant from the engine outlet. These events can be considered disadvantages of a system with a thermostat. Because with the decrease in pressure in the cooling system, the boiling point of the coolant decreases, increasing the risk of boiling in the engine, and due to this boiling, hot spots are observed in certain areas of the engine. The pressures at the engine inlet, radiator inlet, and outlet are shown in Figure 8.

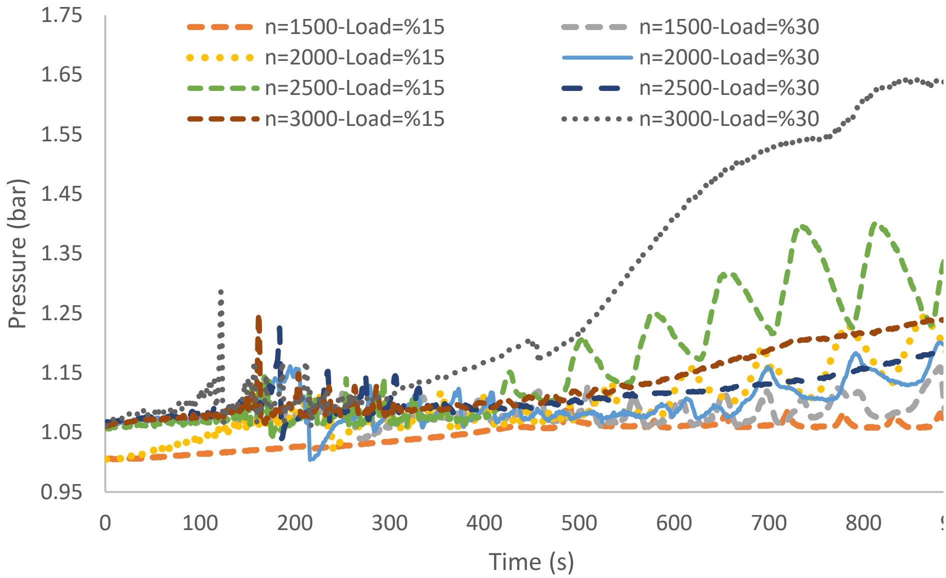
1.75
1.65
1.55
1.45
1.35
1.25
1.15
1.05
0.95
Pressure (bar)
0
100
200
300
400
500
600
700
800
Time (s)
n=1500-Load=%15
n=2000-Load=%15
n=2500-Load=%15
n=3000-Load=%15
n=1500-Load=%30
n=2000-Load=%30
n=2500-Load=%30
n=3000-Load=%30

(a)

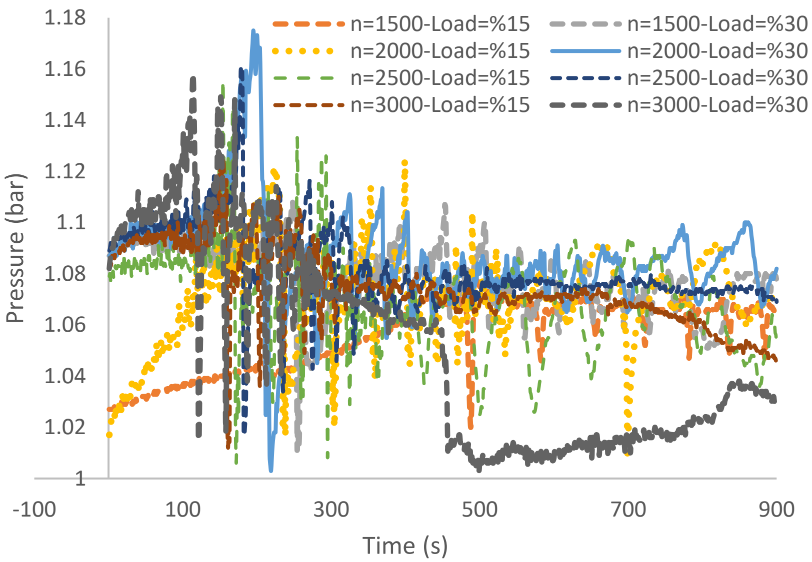
1.18
1.16
1.14
1.12
1.1
1.08
1.06
1.04
1.02
1
Pressure (bar)
-100
100
300
500
700
900
Time (s)
n=1500-Load=%15
n=2000-Load=%15
n=2500-Load=%15
n=3000-Load=%15
n=1500-Load=%30
n=2000-Load=%30
n=2500-Load=%30
n=3000-Load=%30

(b)

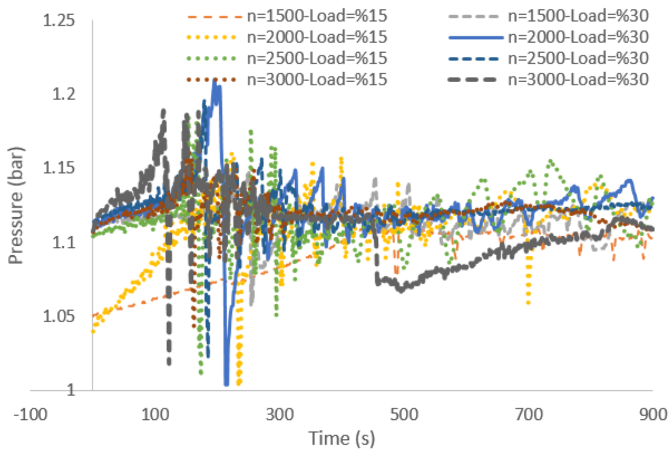

(c)

Figure 8. compares the pressure comparison of the coolant fluid at (a) radiator inlet, (b) radiator outlet, (c) engine inlet.

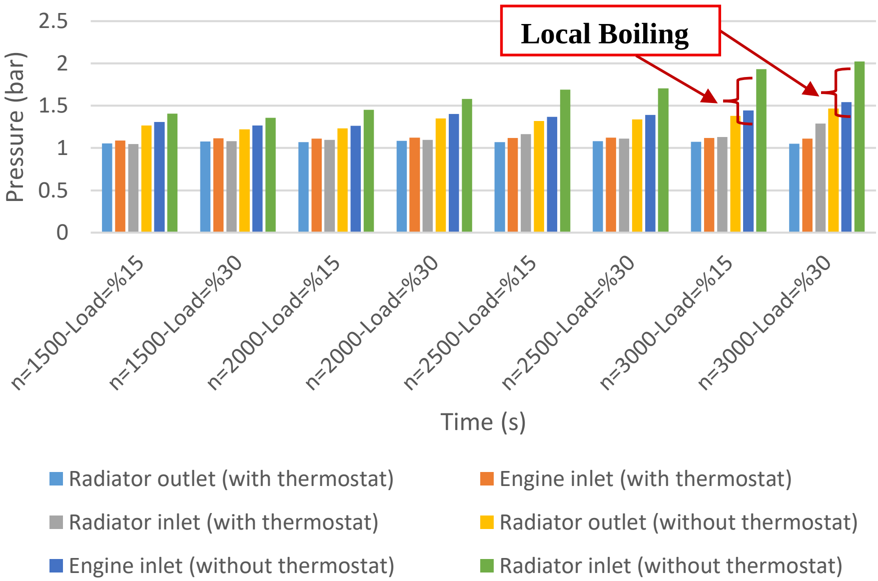

Figure 9. compares the average of the three measured pressures at 15% and 30% load in both thermostat and non-thermostat conditions.

The average pressure of the coolant fluid for both conditions (thermostat system and non-thermostat system) and in all 8 tests is plotted on a graph in

Figure 9. In this chart, the X-axis component represents time, and the Y-axis component represents pressure. This figure examines the pressure variations of three sensors under different speeds and loads. This graph shows that the average pressure measured at all three points for all tests in the non-thermostat condition is higher than in the thermostat condition.

For example, the comparison in the thermostat and non-thermostat conditions at 3000 RPM and 30% load is 59%, 39%, and 38% for the radiator inlet, radiator outlet, and engine inlet, respectively. Therefore, it can be concluded that the pressure difference at the radiator inlet in the non-thermostat condition is the highest compared to the thermostat condition. According to relations 8 to 12, it can be concluded that increasing the speed (rpm) will increase (u), amplification (Re) and (h) and the increase in pressure observed in Figure 9, especially in the case without a thermostat, will be due to higher flow and consequently higher pressure. Based on the histograms in Figure 9, it is observed that there is always a significant pressure difference between the engine inlet and outlet (i.e., the radiator inlet). This increase in the cooling fluid pressure at the engine outlet compared to the inlet can only be attributed to localized boiling occurring in the engine. This pressure difference further intensifies as the engine speed and load increase due to higher fuel consumption, greater heat release, and a corresponding rise in the extent of localized boiling in the engine.

4) Conclusions

The engine cooling system is one of the vital components of internal combustion engines, designed to maintain optimal operating temperatures and prevent overheating. When the engine is running, it generates significant heat, and an efficient cooling system ensures that temperatures remain within safe limits, thereby enhancing performance, reliability, and longevity. This study examined the effect of changes in coolant pressure on local boiling in the Ford MVH418 engine. Tests were conducted at eight different speeds and two loads of 15% and 30%. The Cussons dynamometer was used to measure load and torque. The coolant pressure was measured at three points: the inlet and outlet of the radiator and the engine inlet, using the MPS500 pressure sensor. The results showed that at high RPMs and heavy loads, the warm-up time is shorter. It was also found that the greatest pressure difference in all tests was related to the pressure difference between the inlet and outlet of the radiator, which increases with higher RPMs and applied loads. For example, this pressure difference at 1500 RPM and 30% load is a maximum of 6.10%, which increases to 38.3% at 3000 RPM and 30% load. The addition of a thermostat to the system causes severe pressure fluctuations. In fact, these fluctuations are due to the continuous opening and closing of the thermostat.

Future research should employ advanced diagnostic and modeling tools to deepen understanding of how coolant pressure fluctuations influence localized boiling in engines. Recommended approaches include experiments with advanced coolant formulations such as nanofluids, high-fidelity CFD and transient two-phase flow simulations, and coupled thermal–structural analyses. Additionally, the use of thermal imaging cameras and high-speed visualization is advised to pinpoint localized boiling sites and develop effective mitigation strategies.

References

[1] Rahmatinejad, B., Rahimi Asiabaraki, H., & Azimpour Shishevan, F. (2023). *Investigation of the effect of AL2O3 nanofluid in M13NI engine cooling system*. The Journal of Engine Research, 70(1), 47-65.https://doi.org/10.22034/ER.2023.1975318.0

[2] Ghasemi Zavaragh, H. (2022). *Optimization of the Cooling System of a Gasoline Internal Combustion Engine to Reduce Fuel Consumption and Exhaust Emissions*. *Karafan Journal*, 19(1), 291-309.https://doi.org/10.48301/KSSA.2021.284665.1580

[3] Rahmati Nejad, B., Abbasgholipour, M., & Mohammadi Alasti, B. (2022). *Experimental Evaluation of Heat Transfer of MF 285 Tractor Radiator, using Nano-fluid AL2O3+ Water*. Journal of Agricultural Machinery, 12(3), 281-299.https://doi.org/10.22067/jam.2020.58870.0

[4] Shakeri, A., Keshavarz, A., Qasemian, A., & Moradi, F. (2019). *Simulation of Subcooled Flow Boiling Occurring in Internal Combustion Engine Water Jacket by Numerical Modeling in a Channel with Hot Spot*. The Journal of Engine Research, 53(53), 23-32.

[5] Shabani, F., Khosravi Farsani, A., & Asadi Boroujeni, B. (2022). *Experimental Solution and Numerical Simulation of Flow and Heat Transfer in Car Radiators in Forced and Natural Flows*. Karafan Journal, 19(3), 71-95.https://doi.org/10.48301/KSSA.2022.336734.2061

[6] Alalo, A. M. A., Babaie, M., Shirneshan, A., Bodisco, T. A., Ristovski, Z. D., Brown, R. J., & Zare, A. (2022). *Exergy and energy analysis during cold-start and warm-up engine operation*. Fuel, 330, 125580.https://doi.org/10.1016/j.fuel.2022.125580

[7] Etikyala, S., Koopmans, L., & Dahlander, P. (2023). *Visualization of soot formation in load transients during GDI engine warm-up*. International Journal of Engine Research, 24(7), 3073-3084.https://doi.org/10.1177/14680874221141125

[8] Lee, J., Lee, J., & Lee, K. (2024). *Improving Vehicle Warm-Up Performance Using Phase-Change Materials and Thermal Storage Methods*. Energies, 17(18), 4556.https://doi.org/10.3390/en17184556

[9] Redouane, F., Zineb, C. D., & Rachid, H. (2024). *Vehicle Engine Cooling System: Review Research*. Journal of Nanofluids, 13(3), 625-637.https://doi.org/10.1166/jon.2024.2172

[10] Chang, I., Sun, M., & Edwards, D. (2024). *Advanced Engine Cooling System for a Gas-Engine Vehicle Part I: A New Coolant Flow Control During Cold Start* (0148-7191).https://doi.org/10.4271/2024-01-2414

[11] Akansu, S. O., Tangöz, S., Kahraman, N., İlhak, M. İ., & Açıkgöz, S. (2017). *Experimental study of gasoline-ethanol-hydrogen blends combustion in an SI engine*. International Journal of Hydrogen Energy, 42(40), 25781-25790.https://doi.org/10.1016/j.ijhydene.2017.07.014

[12] Ghasemi Zavaragh, H., Kaleli, A., Solmuş, İ., & Afshari, F. (2021). *Experimental analysis and evaluation of thermostat effects on engine cooling system*. Journal of Thermal Science, 30, 540-550.https://doi.org/10.1007/s11630-020-1264-8